A point mutation in KINDLIN-3 ablates activation of three integrin subfamilies in humans.

Nikolay L.Malinin, Li Zhang, Jeongsuk Choi, Alieta Ciocea, Olga Razorenova, Yan-Quing M, Eugene A. Podrez, Michael Tosi, Donald P. Lennon, Arnold I. Caplan, Susan B. Shurin, Edward F. Plow and Tatiana V. Byzova

## SUPPLEMENTARY METHODS

**Reagents.** Total RNA, genomic DNA purification and one-step PCR kits were purchased from Qiagen and the PCR supermix from Invitrogen. The IODO-GEN Reagent was purchased from Pierce. Rap1A antibodies were from BD Biosciences, actin antibodies from Sigma, mouse polyclonal anti-KINDLIN-3 antibodies were from Novus Biologicals, Anti beta2 alphaX integrin antibodies from ATCC, alphaL from Dako A/S and Chemicon International, anti-beta1, beta2 and beta3 antibodies from Chemicon International, anti-talin, vinculin and alphaIIb integrin antibodies from Santa Cruz Biotechnology; PE conjugated anti-human CD11b/Mac-1 from BD Bioscience, ZyMax Goat anti-Mouse IgG (H+L) FITC conjugate from Zymed, and NIF from Corvas International. Mouse monoclonal anti-CALDAG GEF1 was a gift from Dr.Graybiel A. (MIT). GST-RalGDS fusion construct was kindly provided by Dr. Parise, LV (U North Car). EGFP-KINDLIN-3 fusion was prepared as previously described. The rabbit anti-KINDLIN-3 was prepared by immunizing rabbits with GMKTASGDYIDS peptide-KLH conjugate. Lymphocyte transfections were performed using an Amaxa Biosystems Cell Line Nucleofector kit V from Lonza.

**Microscopy.** *TIRF (Total Internal Reflection Fluorescence) and DIC (Differential Interference Contrast –Nomarski– imaging).* Live cell imaging was performed using a Leica AM TIRF MC System (Leica Microsystems, Wetzlar, Germany) equipped with a climate chamber BL-TIRF/LSM Black (37 $^{0}$C and 5% $CO_2$). Glass bottom microwell Petri dishes (14 mm microwell, No. 1.5 coverglass from MatTek) were coated with human plasma fibronectin (10 μg $cm^{-2}$) or fibrinogen (200 μg $ml^{-1}$). For live-imaging of cell spreading, cells were transfected with the indicated construct (KINDLIN-3 fusion with EGFP) for 24–48 hours. After PMA stimulation for one hour to induce adhesion, unbound cells were removed by gentle washing. Cells were then sealed in a live-imaging

chamber and moved with a motorized stage. DIC and TIRF images were taken using a 100 X HCX PL APO lens and 1.64 N.A. oil immersion objective and at 488 nm excitation.

**Adhesion assays.** For adhesion of PMN or immortalized lymphocytes, the cells were added to fibrinogen or fibronectin coated plates (1mg $ml^{-1}$) in serum-free media and stimulated with 200 nM PMA for 1hr as described[1]. Plates were washed twice with media, and images were acquired on a Leica DM IRB microscope equipped with a Qimaging camera and QCapture Pro ver.5.1. software. Cell counts per field were scored using NIH Software ver.1.63 in four random fields per well. For platelet adhesion and imaging, gel-filtered platelets ($2x10^7$ $ml^{-1}$) from subjects and control healthy subjects were stimulated by 100 nM PMA and added to coverslips coated with 100 μg $ml^{-1}$ fibrinogen. Attached platelets were stained with phalloidin-Texas Red or anti-αIIbβ3 antibodies followed by secondary antibodies conjugated with Alexa 488. The numbers of attached and spread platelets were counted using a fluorescence microscope.

**Fibrinogen binding and FACS analyses**. To analyze fibrinogen binding by fluorescence-activated cell sorting (FACS), platelets were stimulated as indicated, followed by D-phenylalanyl-L-prolyl-L-argininechloromethyl ketone (PPACK) 5μg $ml^{-1}$; and fluorescein isothiocyanate (FITC)-labeled fibrinogen was added at a final concentration of 300 nM for 30 minutes as described [2]. To analyze PAC-1 and P-selectin expression, gel-filtered platelets were incubated with FITC-labeled PAC-1 or FITC-labeled anti-P-selectin (BD Biosciences) antibodies (10 μg $ml^{-1}$ each) for 30 minutes. FACS was performed using a FACSCalibur (BD Biosciences), and data were analyzed using the manufacturer's CellQuest software program. For DTT-induced fibrinogen binding, aliquots (100 μl) of the cells ($10^5$ $ml^{-1}$) were incubated with FITC-fibrinogen. Untreated cells, DTT (10 mM), DTT and EDTA (10 mM), DTT and cyclic RGD (20 μg $ml^{-1}$) samples were prepared in triplicates. After one hour at 37°C, the cells were washed with PBS and analyzed by FACS using a FACSCanto instrument and FACSDiva ver.6.0 software. For radiolabeled fibrinogen binding, $2\times10^8$ platelets $ml^{-1}$ in presence of $^{125}$I-fibrinogen (10 μCi $mg^{-1}$) were activated with thrombin (1 U $ml^{-1}$) for 15 min. The platelets were separated from unbound $^{125}$I-fibrinogen by centrifugation, and bound fibrinogen quantified in a gamma counter. Non-specific binding – amount of $^{125}$I-

fibrinogen bound to control platelets without thrombin stimulation- was subtracted to calculate specific binding.

**Lymphocyte and granulocyte functional assays.** *Adhesion.* Normal and subject lymphocytes or PMN were purified as described elsewhere and stimulated with 0.16 μM PMA or 1 μM fMLP in HBSS containing 1mM $Ca^{2+}$ and 1mM $Mg^{2+}$ and then incubated at 37°C. The cells ($10^7$) were stirred in a siliconized cuvette in Chrono-log aggregometer, and light transmission was recorded for 20 min. The micrographic pictures shown were taken at 25 min incubation. *Oxidative burst measurement* Superoxide generation was measured by detection of lucigenin chemiluminescence. Samples of PMN treated as indicated at 37°C for 5 min prior to addition of lucigenin (Sigma). Superoxide production was monitored in a aggregometer following addition of lucigenin, calcium and magnesium as described [3]. *NIF binding.* Neutrophil Inhibitory Factor (NIF) was provided by Corvas International, radiolabeled with $^{125}I$ and its binding to PMN was measured as previously described.

**Rap1A activation assay.** Rap1A activation was measured as described elsewhere[4]. Briefly, 2.5x$10^6$ cells were lysed in 500 μl buffer (25 mM HEPES pH 7.6, 500 mM NaCl, 1% NP-40, 2.5 mM $MgCl_2$, 1% glycerol and protease inhibitor cocktail (Roche), and cleared by centrifugation at 12,000xg for 10 min at 4°C. Supernatant fractions were incubated with 30 μl of a 50% slurry of Sepharose-Glutathione beads (Sigma) with pre-bound GST-RalGDS (0.15 mg $ml^{-1}$) for 1h +4°C. Beads were then washed 3 times with the binding buffer, and bound protein was analyzed by SDS-PAGE, followed by transfer and Western blots with anti-Rap1A antibody (BD Biosciences).

**Platelet aggregation**. Platelets were isolated from platelet-rich plasma by gel filtration as described previously [5]. Platelet aggregation stimulated by 10 μM ADP, 100 nM PMA, or thrombin (1 U $ml^{-1}$) was monitored using a Lumi-Aggregometer 500 VS (Chrono-Log).

**Bone Marrow Culture.** Samples of human marrow were rinsed with Dulbecco's Modified Eagle's Medium (DMEM-LG) supplemented with 10% fetal bovine serum (FBS) from a lot selected for expansion and differentiation of human mesenchymal stem cells (hMSC). The marrow cells were then centrifuged on a Percoll gradient as described previously[6 7] . Cells from the top 10 ml of the gradient were collected and seeded into 100-mm tissue culture dishes at a density of 10x$10^6$ cells per dish; additional single

dishes were seeded at densities of 5 and $1x10^6$ for determination of the number of colonies. Cells were continued in primary culture for 14 days when they were subcultured with trypsin-EDTA[7] . Cells were continued in first passage for an additional 7 days when they were again subcultured. The resulting second passage hMSCs were then used in both *in vivo* and *in vitro* assays for osteogenesis. Differentiation of hMSCs along osteogenic pathways *in vitro* was induced as described elsewhere [8]. Cells were seeded at a density of 3,000 $cm^{-2}$ in serum-supplemented medium. On day 1 of 2nd passage, culture medium was further supplemented with ascorbic acid 2 -phosphate (control condition) or with ascorbic acid 2-phosphate and $10^{-7}$M dexamethasone (osteogenic supplements (OS). Beginning on day 10 of 2nd passage, medium for each of these conditions was further augmented with 10mM β-glycerophosphate.

***In Vivo* Ceramic Cube Assay.** Second passage cells were loaded into porous tricalcium phosphate/hydroxyapatite ceramic cubes previously coated with fibronectin[9]. hMSC from the marrow of a healthy donor were also loaded into cubes and used as a positive control. The loaded cubes were implanted into immunocompromised mice; both nude mice and SCID mice were utilized. Host animals were sacrificed at 3 and 6 weeks. The cubes were harvested, fixed in 10% buffered formalin, embedded in paraffin and cut into sections 7μm thickness. Alternate sections were stained with toluidine blue or Mallory-Heidenhain. Stained slides were evaluated by brightfield optics with an Olympus IMT-2 inverted microscope. Each histologic section was given a score of between 0 and 4 based on the abundance of bone and cartilage. Scores of 1, 2, 3, and 4 indicated, respectively, that up to 25, 50, 75, or 100% of the pores in an individual section of a ceramic cube contained bone or cartilage. An overall score for a cube was determined by calculating the average score for all sections[9]. In contrast to cubes loaded with control cells or with post-transplantation cells from the same subject, cubes that had been loaded with cells from subject before bone marrow transplantation contained abundant cartilage and "fibrocartilage" in addition to bone and fibrous tissue. The presence of cartilage in ceramic cubes loaded with human MSCs and implanted in immunocompromised mice is extremely unusual and is virtually never seen in this assay.

**Calcium Assay.** Total cellular calcium accumulation was determined for cultures from subject after bone marrow replacement on day 23 of second passage, and for cultures from subject before bone marrow replacement on day 21 of fourth passage; control and

OS cultures were assayed in each case as described[9]. Calcium values were higher for OS cultures than for control cultures in cells from both marrow harvests, as well as in cells derived from a healthy volunteer donor, which served as a positive control. In each case, however, the cells responded to osteogenic supplements by increasing the level of alkaline phosphatase activity. The high calcium levels for the cells from subject 2 were also evident in von Kossa staining. Cultures exposed to osteogenic supplements developed large areas of black punctate staining, indicating the presence of mineralized deposits in association with multilayered cell aggregates.


1. Byzova, T.V.*, et al.* A mechanism for modulation of cellular responses to VEGF: activation of the integrins. *Mol Cell* **6**, 851-860 (2000).
2. Zamarron, C., Ginsberg, M.H. & Plow, E.F. A receptor-induced binding site in fibrinogen elicited by its interaction with platelet membrane glycoprotein IIb-IIIa. *J Biol Chem* **266**, 16193-16199 (1991).
3. Freedman, J.E. & Keaney, J.F., Jr. Nitric oxide and superoxide detection in human platelets. *Methods Enzymol* **301**, 61-70 (1999).
4. Franke, B., Akkerman, J.W. & Bos, J.L. Rapid Ca2+-mediated activation of Rap1 in human platelets. *EMBO J* **16**, 252-259 (1997).
5. Byzova, T.V. & Plow, E.F. Networking in the hemostatic system. Integrin alphaiibbeta3 binds prothrombin and influences its activation. *J Biol Chem* **272**, 27183-27188 (1997).
6. Solchaga, L.A., Welter, J.F., Lennon, D.P. & Caplan, A.I. Generation of pluripotent stem cells and their differentiation to the chondrocytic phenotype. *Methods Mol Med* **100**, 53-68 (2004).
7. Lennon, D.P. & Caplan, A.I. Isolation of rat marrow-derived mesenchymal stem cells. *Exp Hematol* **34**, 1606-1607 (2006).
8. Lennon, D.P., Bruder, S.P., Haynesworth, S.E., Jaiswal, N., and Caplan, A.I. Human and Animal Mesenchymal Progenitor Cells From Bone Marrow: Selection of Serum for Optimal Proliferation. *In Vitro Cell and Develop. Biol.* **32**, 602-611 (1996).
9. Dennis, J.E., Konstantakos, E.K., Arm, D. & Caplan, A.I. In vivo osteogenesis assay: a rapid method for quantitative analysis. *Biomaterials* **19**, 1323-1328 (1998).

Supplementary Figure 1

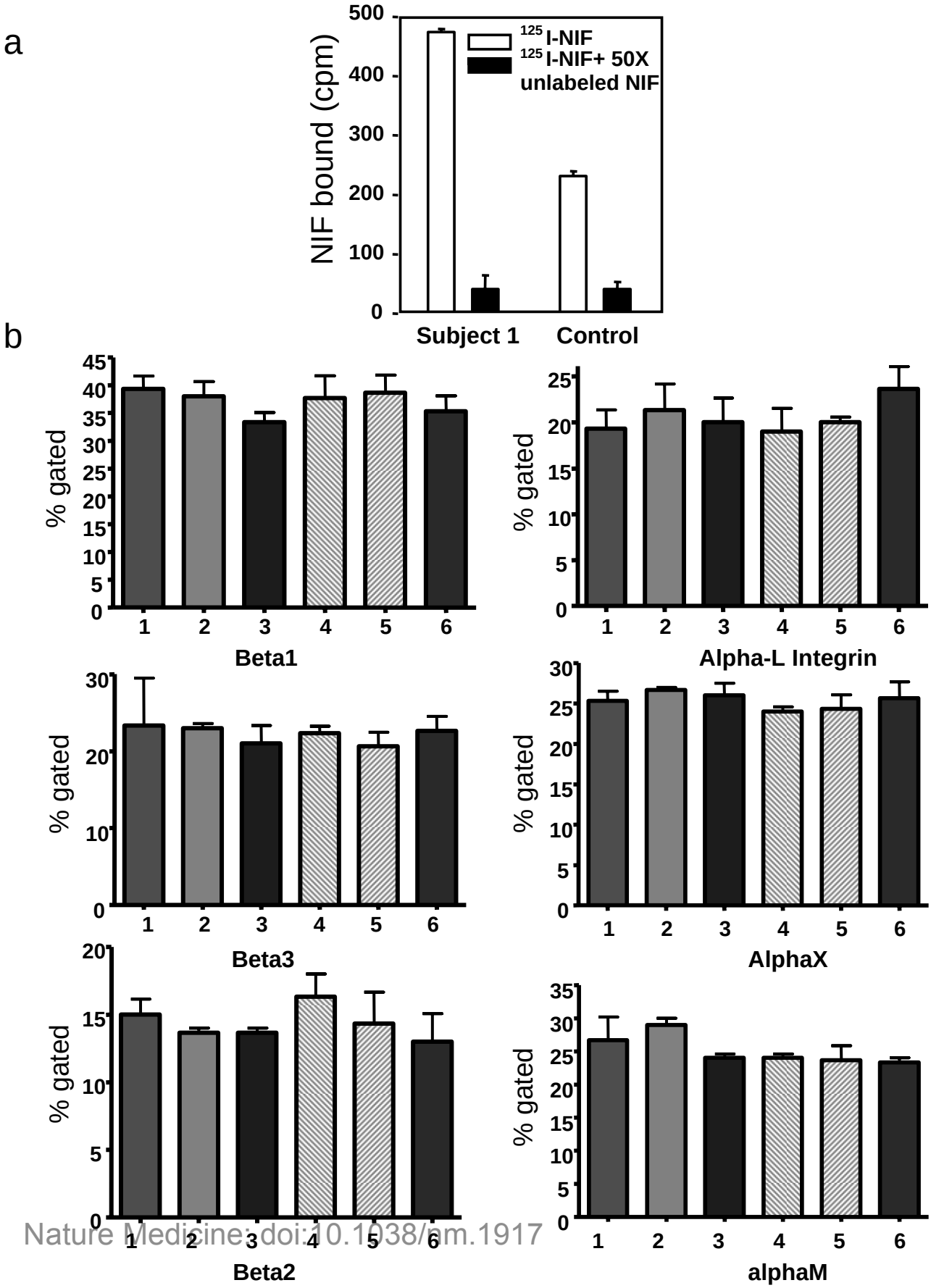

**Supplementary Fig. 1** Expression levels of integrins on subjects and healthy control cells. **a.** NIF binding to subject's and control cells. $^{125}$-I labeled NIF binding was measured as described in Methods. Total binding is inhibitable by more then 100 fold by 50X excess of unlabeled NIF. Note that subject cells bind more NIF, which serves as an activation-independent ligand for αmβ2 integrin. **b.** Expression of individual integrin subunits (beta 1, alpha L, beta 3, alpha X, beta 2 and alpha M) expression on EBV-transformed subjects', parents' and control cells and K562 cell line was performed using flow cytometry. The means ±SD of % gated cell populations from three experiments are shown. 1 - Parent (Subject F); 2 - Parent (Subject M); 3 – normal control; 4- Subject 1; 5 - Subject 2; 6 - K652 cell line. There was no significant difference between samples.

Supplementary Figure 2

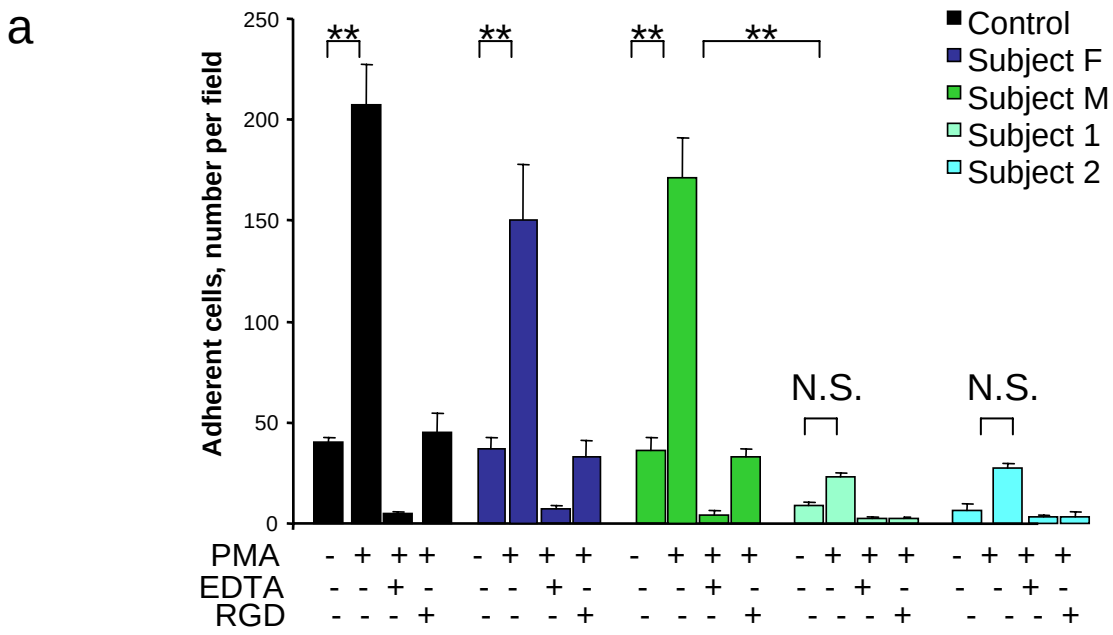


b

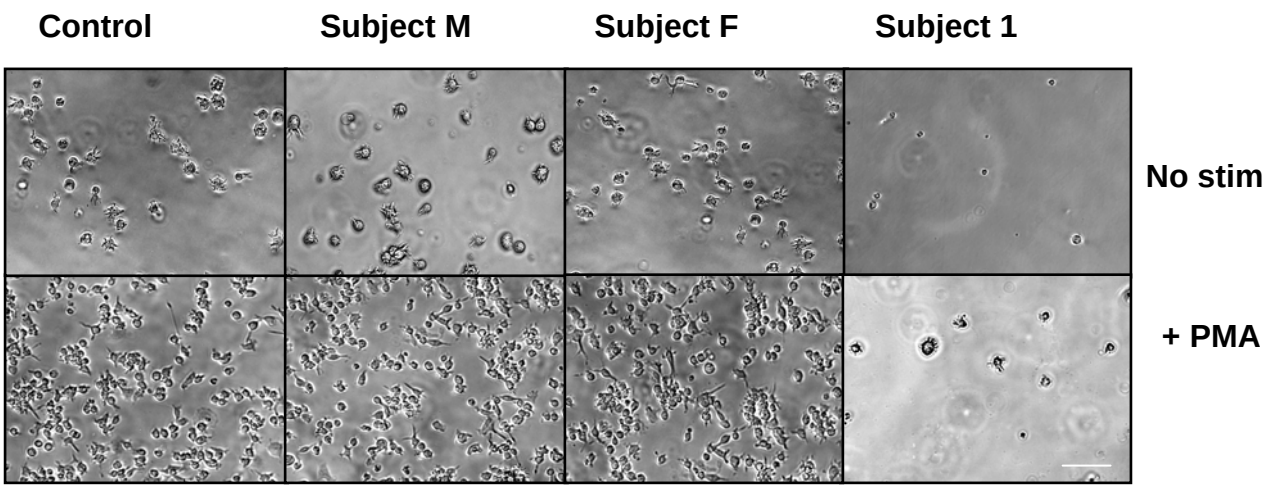


Nature Medicine: doi:10.1038/nm.1917

Supplementary Figure 2

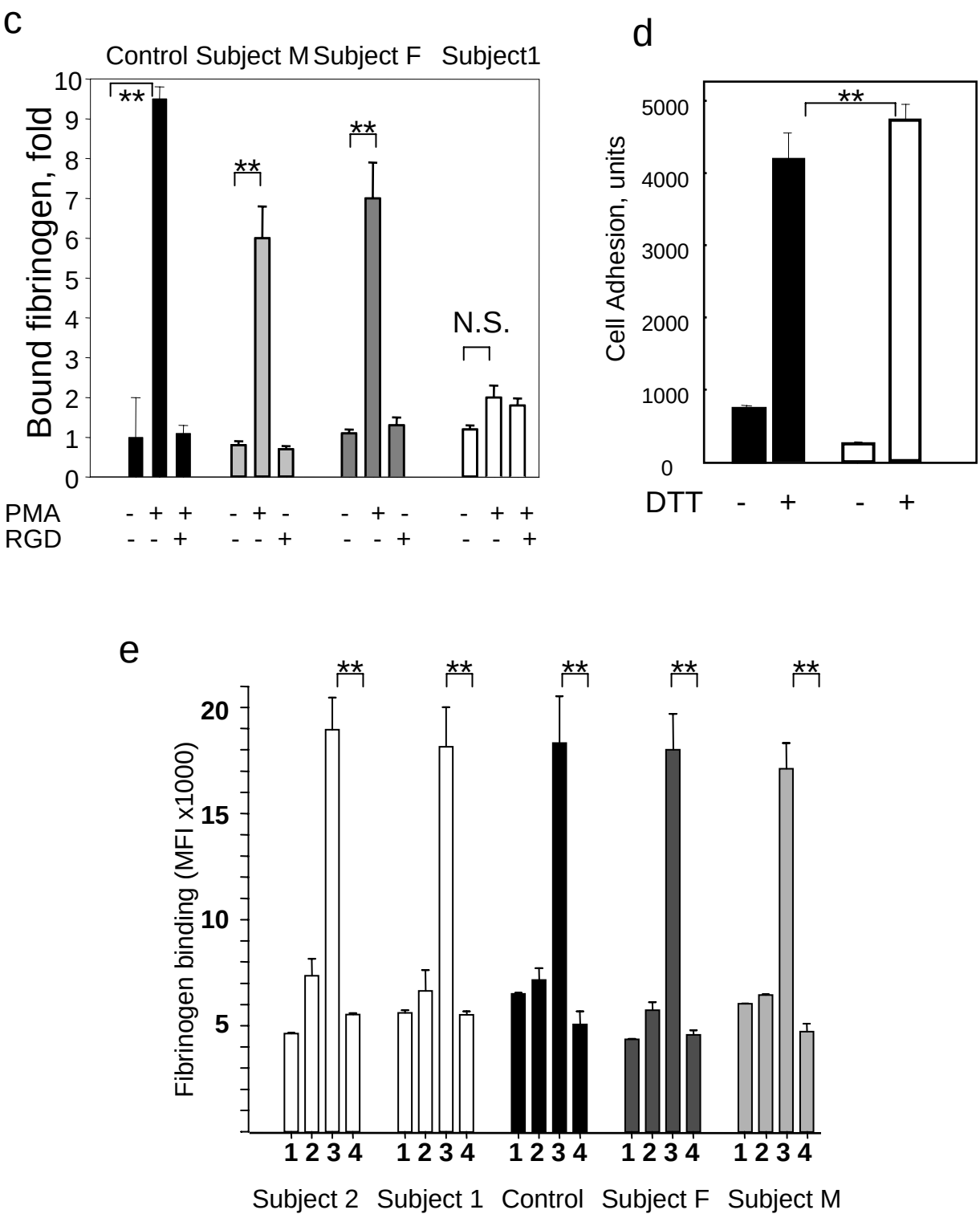


Nature Medicine: doi:10.1038/nm.1917

**Supplementary Fig. 2** Deficiency of integrin activation by inside-out signaling. **a.** Peripheral blood mononuclear cells were isolated from blood of healthy control, two subjects and their parents and immortalized as described in Methods. Adhesion of immortalized cells to fibronectin was quantified as described in Methods in the presence or absence of 200 nM PMA, 1mM EDTA and 200 μM RGD peptide as indicated. Data represent means± SD; n=5; $^{**}P<0.01$, N.S. not significant. **b.** Representative images of adhered cells from 2a. Light-field microphotographs of adherent EBV-transformed cells from subject, parents and healthy control on fibrinogen substrate are shown. Note the complete lack of subject's cell adhesion Scale bar 50 μM. **c.** Soluble fibrinogen binding to control, parents' and subject's cells in suspension was measured by FACS as described in Methods. Cells were stimulated by 200 nM PMA as indicated. Nonspecific (integrin-independent) binding was measured in the presence of 200 μM RGD peptide as indicated. Fold increase over control are shown. Fibrinogen binding to unstimulated control cells was assigned a value of 1. The data represent means±SD (n=4; $^{**}P<0.01$, N.S. not significant). **d. A**dhesion of primary control (black bars) and subject's (white bars) lymphocytes to fibrinogen in the presence of DTT**.** Calcein-labeled lymphocytes were pre-treated with 50 mM DTT, added to the plates, incubated and washed as described in Methods. Cell adhesion is shown in fluorescence units (data means±SD, n=4; $^{**}P<0.01$, N.S. not significant). **e.** Binding of FITC-labeled fibrinogen to subjects' and control cell lines in the presence of 10 mM DTT as described in Methods. Cells were treated as follows: 1 - DTT plus EDTA; 2 – DTT plus 200 μM RGD peptide; 3- DTT alone; 4 – no treatment. MFI -stands for mean of fluorescence intensity. The data represent means±SD (n=4; $^{**}P<0.01$, N.S. not significant).

Supplementary Figure 3

a

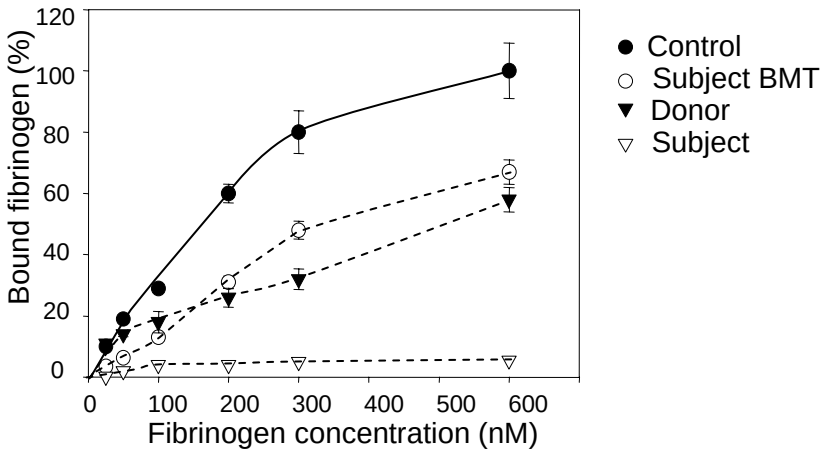


b

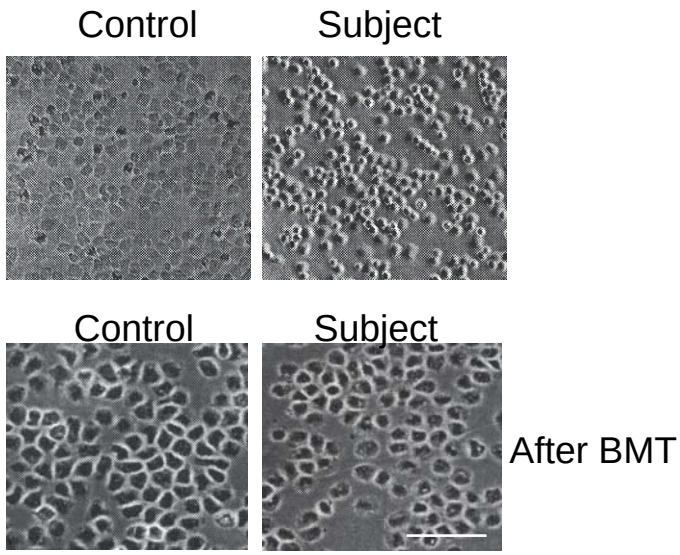


Nature Medicine: doi:10.1038/nm.1917

**Supplementary Fig. 3** Platelets and neutrophils adhesion is restored after bone marrow transplantation. **a.** Fibrinogen binding to platelets isolated from healthy controls (filled circles), subject (open triangles), bone marrow donor for the subject (paternal uncle) (filled triangles) and subject after bone marrow replacement (open circles). Platelets were isolated, stimulated with 20 μM ADP and incubated with indicated concentrations of radiolabeled fibrinogen. Bound fibrinogen was quantified as described in Methods. Specific binding is shown. Amount of bound fibrinogen to control platelets at 600 nM of added fibrinogen was assigned a value of 100%. **b.** Adhesion and spreading of neutrophils isolated from healthy controls and subject before and after bone marrow replacement. Denatured ovalbumin was used as a substrate. Scale bar 30μm.

Supplementary Figure 4

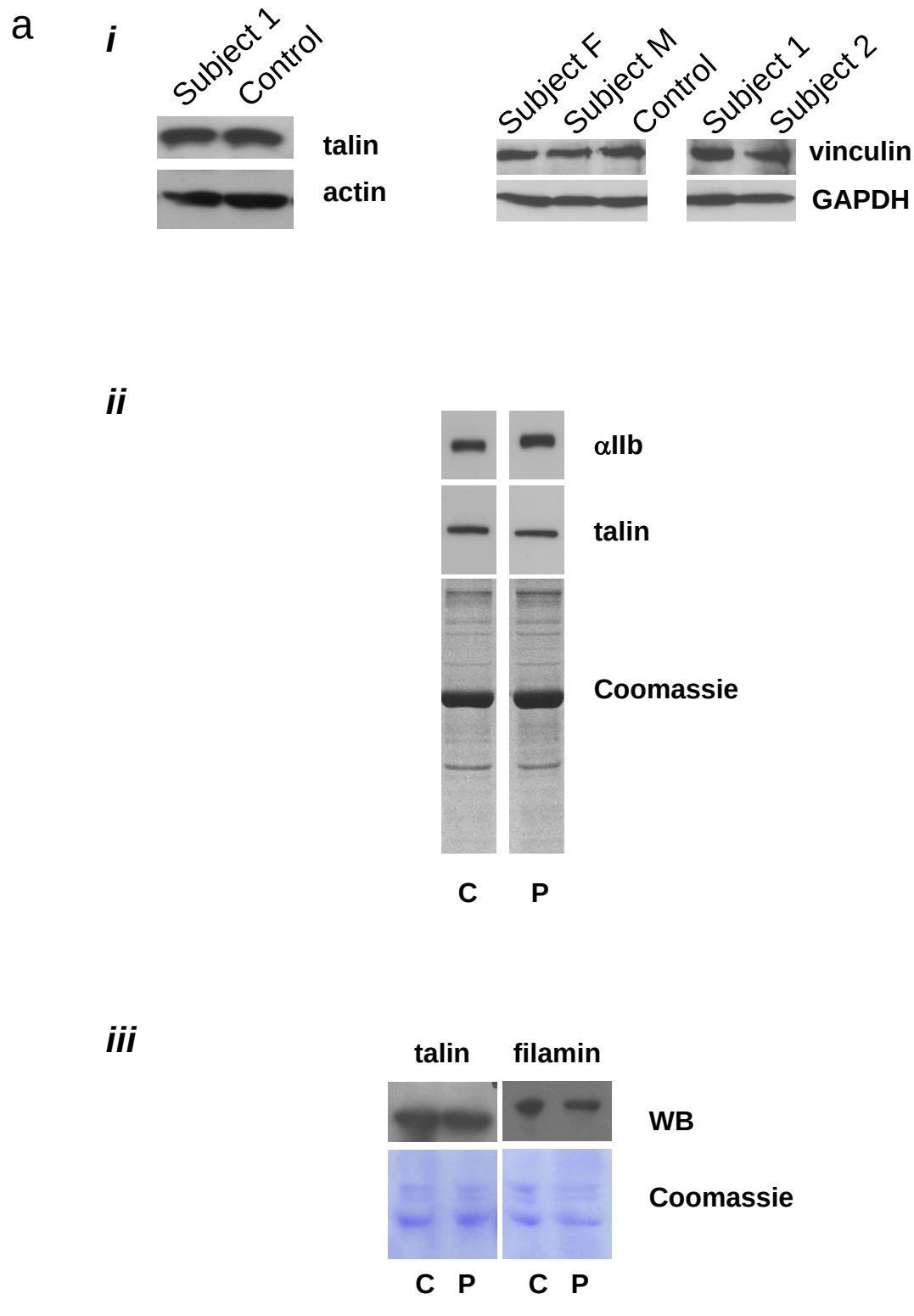


Nature Medicine: doi:10.1038/nm.1917

Supplementary Figure 4

b

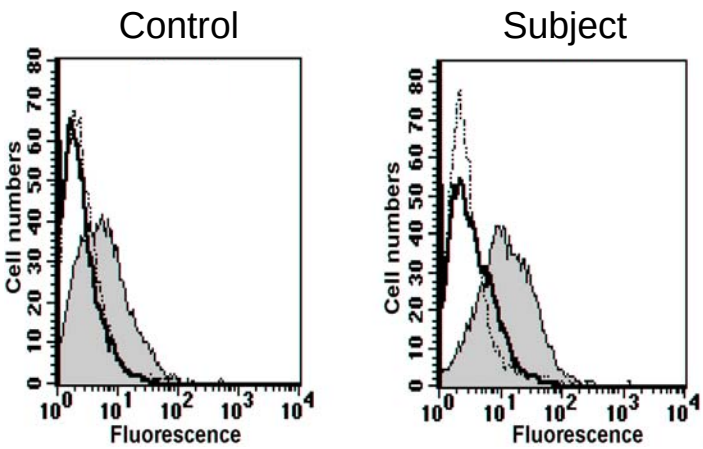


c

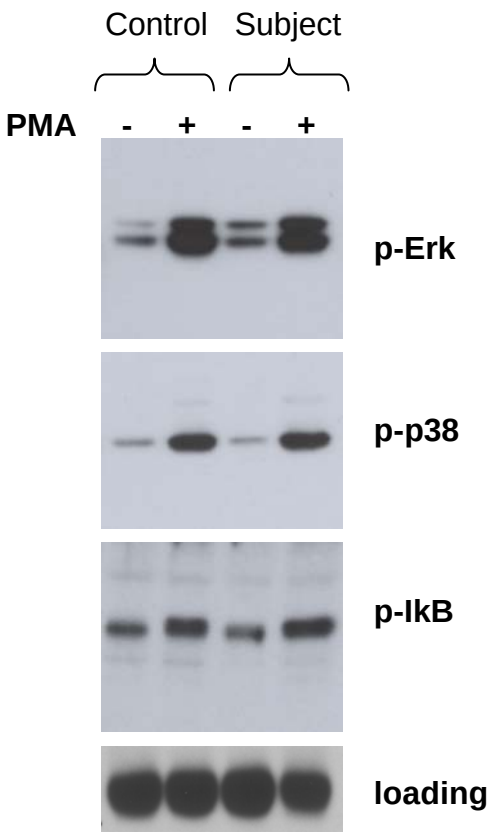


Nature Medicine: doi:10.1038/nm.1917

**Supplementary Fig. 4** PMA-induced signaling and talin expression are normal in subject's cells **a.** Talin, vinculin and filamin expression. *i*. Presence of talin and vinculin in EBV-transformed cells from control and subject. Actin and GAPDH were used as loading controls for talin and vinculin, respectively. *ii*. and *iii*. alphaIIb integrin, talin, and filamin expression in subject platelets (before BMT) c - control, p - subject. Coomassie-stained gels loaded with the same samples were used to demonstrate equal loading. **b.** The subject's and normal control primary lymphocytes were incubated with buffer alone (solid line with shade) or PMA (solid line without shade), and analyzed for L-selectin expression by FACS analysis using L-selectin specific mAb. The dotted line represents negative control using an isotype matched and irrelevant mAb. **c.** Signaling pathways induced by PMA are not impaired in subjects' cells. Cells were treated with PMA, lyzed, subjected to SDS-PAGE with subsequent Western blotting. Blots were probed with phospho-specific anti- ERK, p38 and IkappaB antibodies as indicated.

Supplementary Figure 5

a

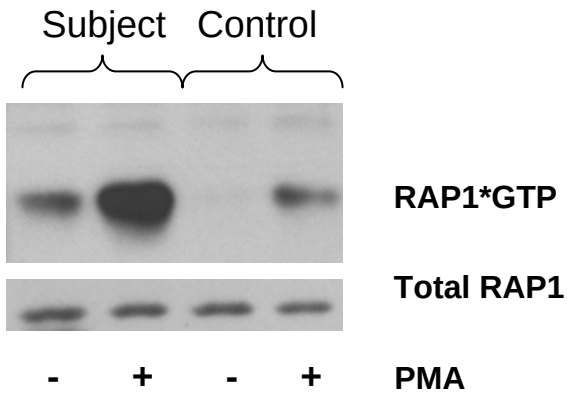


b

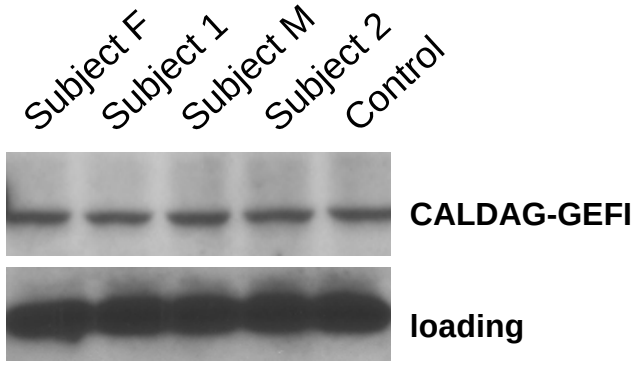


c

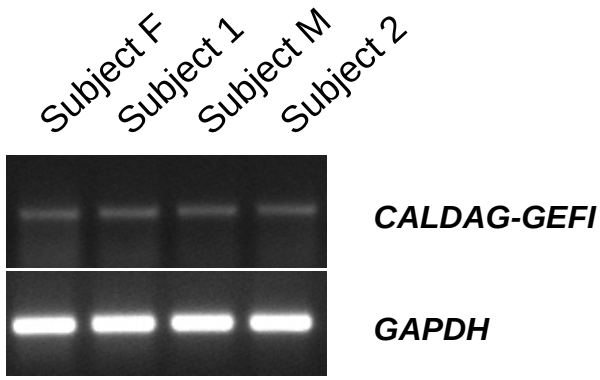


Nature Medicine: doi:10.1038/nm.1917

**Supplementary Fig. 5** Rap1 activation and CALDAG GEFI expression are intact in subject's cells. **a.** Rap1 activation in response to PMA is elevated in subject's cells. Western blot of GST-RalGDS pull-down assay and whole cell lysates were subjected to SDS-PAGE with subsequent Western blotting. Blots were probed with anti-Rap1 antibodies. **b–c.** CALDAG-GEFI (RASGRP2) expression levels are similar in subjects', parental and control cells. **b.** Cellular lysates were subjected to SDS-PAGE with subsequent Western blotting using mouse monoclonal anti-CALDAG-GEF1 antibodies. **c.** Semi-quantitative RT-PCR using total RNA isolated from EBV-transformed cells (both subjects and both parents) as described in Methods.

# Supplementary Figure 6

a

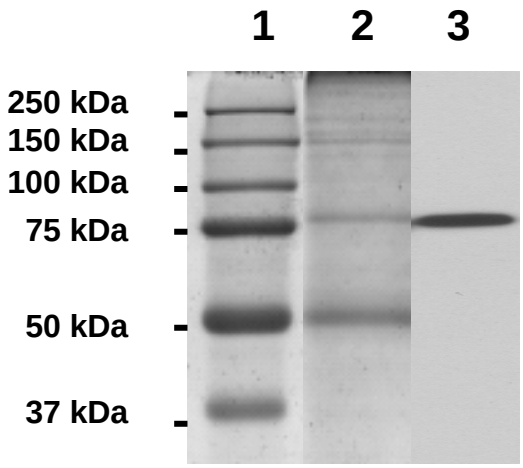


b

```
  1 MAGMKTASGD YIDSSWELRV FVGEEDPEAE SVTLRVTGES HIGGVLLKIV
 51 EQINRKQDWS DHAIWWEQKR QWLLQTHWTL DKYGILADAR LFFGPQHRPV
101 ILRLPNRRAL RLRASFSQPL FQAVAAICRL LSIRHPEELS LLRAPEKKEK
151 KKKEKEPEEE LYDLSKVVLA GGVAPALFRG MPAHFSDSAQ TEACYHMLSR
201 PQPPPDPLLL QRLPRPSSLS DKTQLHSRWL DSSRCLMQQG IKAGDALWLR
251 FKYYSFFDLD PKTDPVRLTQ LYEQARWDLL LEEIDCTEEE MMVFAALQYH
301 INKLSQSGEV GEPAGTDPGL DDLDVALSNL EVKLEGSAPT DVLDSLTTIP
351 ELKDHLRIFR IPRRPRKLTL KGYRQHWVVF KETTLSYYKS QDEAPGDPIQ
401 QLNLKGCEVV PDVNVSGQKF CIKLLVPSPE GMSEIYLRCQ DEQQYARWMA
451 GCRLASKGRT MADSSYTSEV QAILAFLSLQ RTGSGGPGNH PHGPDASAEG
501 LNPYGLVAPR FQRKFKAKQL TPRILEAHQN VAQLSLAEAQ LRFIQAWQSL
551 PDFGISYVMV RFKGSRKDEI LGIANNRLIR IDLAVGDVVK TWRFSNMRQW
601 NVNWDIRQVA IEFDEHINVA FSCVSASCRI VHEYIGGYIF LSTRERARGE
651 ELDEDLFLQL TGGHEAF
```

Nature Medicine: doi:10.1038/nm.1917

# Supplementary Figure 6

c

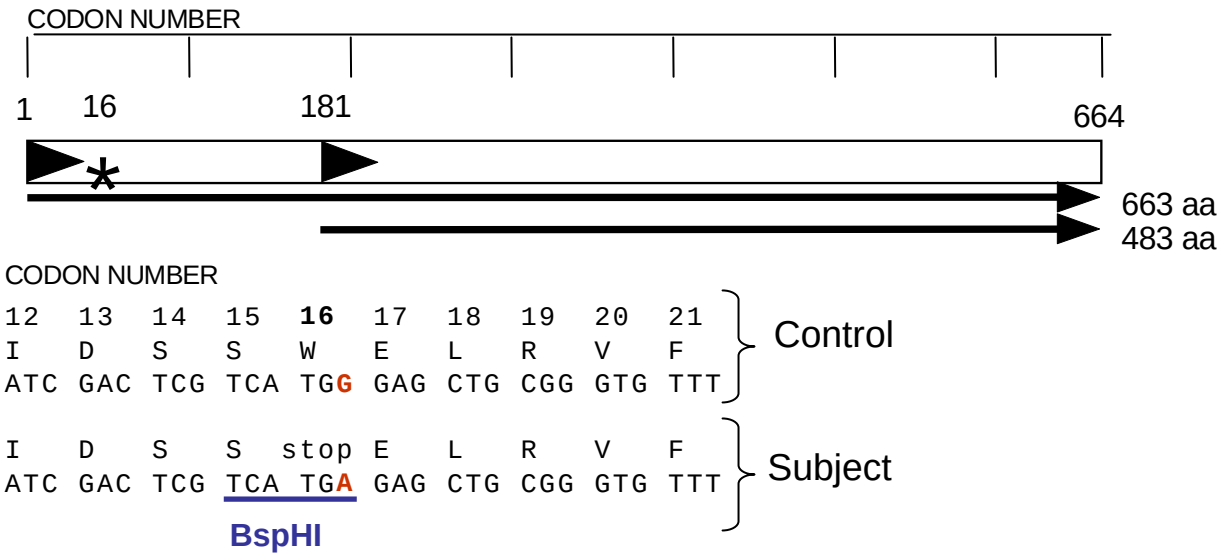


d

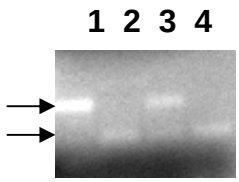


Nature Medicine: doi:10.1038/nm.1917

**Supplementary Fig. 6** Detection of mutated *KINDLIN*-3. **a.** Enriched p75 (KINDLIN-3) sample was subjected to Mass-Spectroscopy analysis. 1 and 2: Gel stained with Deep purple: lane 1- molecular weight marker, lane 2 - sample enriched in KINDLIN-3. Lane 3- Sample as in 2 was probed on Western blotting using anti-KINDLIN-3 antibodies. **b.** Peptide coverage of KINDLIN-3 from the sample discussed in **a**. Matched peptides are shown in red. Sequence coverage was 68%. **c.** Schematic representation of *KINDLIN*-3 (*FERMT3*) ORF is shown. Codon numbers are indicated on top, position of the mutation is shown with an asterisk. Initiation ATG and alternative initiation ATG are indicated with triangles. Length of original protein and the mutated form are shown below. Nucleotide and protein sequence around the mutated site are shown. New *Bsp*HI restriction site formed as the result of the mutation is underlined. **d.** Agarose gel of *Bsp*HI-cut *KINDLIN*-3 genomic PCR product (175 bp, corresponding to the second exon of human gene as described in Methods). Lanes: (1) Non-mutated gene from healthy control gives a single 175 bp band; (2 and 4) Mutated gene in subjects: lane 2 - subject 1; lane 4 - subject 2. Note the presence of the single restriction site, which results in the generation of two products: 116 and 59 bp. Lower band is masked by the dye. (3) Both alleles are present in parent (subject F). Note PCR product of 175 bp (as in normal control sample shown in lane 1) and 116 bp and 59 bp (lower band is masked).

**Supplemental Note.**

Additional details of subjects' medical history.

The two siblings, a boy (subject 1) and a girl (subject 2) presented with recurrent clinical bleeding and infections by two weeks of age. Family history was negative, including recurrent infections and bleeding. All pregnancies were uncomplicated and full term. The parents are native to the United Arab Emirates and had an older son with no medical problems. Both parents had normal platelet and neutrophil function.

For both siblings, the most severe clinical manifestation of their disease was mucocutaneous bleeding. Recurrent infection was evident in both subjects, but not the most severe manifestation. The presence of hemosiderin-laden macrophages on several bronchoalveolar lavages performed on both children suggested that the recurrent pulmonary infiltrates were due predominantly to pulmonary hemorrhage rather than infections. Both subjects had normal platelet counts, hemoglobin levels, and peripheral blood cell morphology. Both had leukocyte counts ranging between 35 and 70 x $10^9$/l, approximately equal numbers of neutrophils and lymphocytes, without immature myeloid or lymphoid forms. The only finding on physical examination was hepatosplenomegaly in both subjects. Chronic leukocytosis, failure of cells to manifest complement mediated functions, splenomegaly and osteopetrosis were all clinically consistent with leukocyte adhesion deficiency I (LAD-1). Characterization of the cellular defects did not support a diagnosis of any known integrin defect of either platelets or neutrophils.

*Subject 1* –At presentation at University Hospitals of Cleveland at 7 months of age, cardiac, hepatic, renal function and imaging were all normal. Bronchoalveolar lavage was performed and yielded hemosiderin-laden macrophages and no pathogens. The subject's head circumference was at the 97$^{th}$ percentile, his liver span was 13 cm, spleen 8 cm below the left costal margin (confirmed hepatosplenomegaly), and lymph nodes were not enlarged. Malarial parasites were noted on peripheral blood smear, for which the subject was treated. After treatment, erythrocyte numbers and morphology were normal. Prothrombin and activated partial thromboplastin times were normal. Bleeding time exceeded 23 minutes. Detailed neuropsychological testing was completely normal.

*Subject 2*- At evaluation at University Hospitals of Cleveland at 5 months of age, cardiac, hepatic and renal functions were normal, as were growth and development. This subject

developed mucocutaneous bleeding at two weeks of age. She also had hepatosplenomegaly. Diffuse interstitial infiltrates and hemosiderin-laden macrophages were present in bronchoalveolar lavages. Skeletal survey showed osteopetrosis. She had multiple episodes of mucocutaneous bleeding, which responded to platelet infusions. She experienced intracranial hemorrhage at four months.

Bone marrow transplantation in subject 1 and 2.

Because of the frequency and severity of bleeding, both subjects underwent allogeneic bone marrow transplantation.

*Subject 1*. The parents shared HLA antigens, but neither matched subject 1. A paternal uncle was found to be a 6 antigen match. His medical history and detailed studies of hematopoietic cell function were all normal. Thus, the paternal uncle served as a donor of bone marrow for subject 1. Allogeneic hematopoietic stem cell transplant was performed with full engraftment. No acute graft-versus-host disease (GvHD) was noted, but after return to the UAE, the child developed chronic GvHD.

As a result of bone marrow transplantation, the osteopetrosis has resolved, and neither infection nor bleeding has recurred since the resolution of chronic GvHD.

*Subject 2* received hematopoietic stem cells from her 6 antigen-matched maternal donor. Cellular function was normal in the mother and in the grafted hematopoietic cells transplanted into the daughter. No mucocutaneous bleeding occurred after engraftment of donor cells. Subject 2 developed acute GvHD, which resolved.

Thus, bone marrow transplantation resolved all of the overt clinical problems in both subjects.

Movie legends

Movie 1 of subject's cells transfected with control GFP vector. Differential Interference contrast (DIC) and fluorescence are shown. Frames were recorded every 5 seconds. Subject's cells float but fail to adhere to fibronectin.

Movie 2 of subject's cells transfected with kindling-3-GFP fusion construct. Differential Interference contrast (DIC) and fluorescence are shown. Frames were recorded every 5 seconds. Upon expression of KINDLIN-3, subjects cells attach and spread on fibronectin. Note raffles formation and active movement of KINDLIN-3 overexpressing cells. Movies of representative cells are shown.